Proceedings of the
Annual Stability Conference
Structural Stability Research Council
Louisville, Kentucky, April 13-16, 2021

The effect of transverse stiffeners and end-plates on the lateral-torsional buckling of beams

Trung Hoang[1], Sándor Ádány[2]

Abstract
In this paper the effect of transverse stiffeners on the lateral-torsional buckling of thin-walled beams is discussed. First, an analytical solution is presented for the critical moment associated with the lateral-torsional buckling in the case of doubly-symmetrical I-section beams with some simple support conditions. The effect of the transverse plate elements is directly considered, by using the energy method. The analytical solutions, then, are compared to shell finite element solutions, using a general purpose finite element software as well as the constrained finite element method, which has recently been extended to handle members with transverse plate elements. The results well illustrate that the effect of the transverse plate elements is two-fold. One effect is that the deformations of the transverse elements contribute to the potential energy, hence increase the critical load. The other effect is that the transverse plates modify the buckled shape of the member, which also modifies the critical load. Though the analytical solutions are found to be reasonably precise for a number of cases, their applicability is limited. Still, the analytical solutions are helpful in understanding how the transverse elements influence the behavior. Moreover, the results suggest that the transverse stiffeners have a beneficial, and sometimes considerable effect on the critical moment, which effect could be considered also in the design.

1. Introduction

Lateral-torsional buckling (LTB) is a potential, and frequently governing failure mode of unrestrained or partially restrained thin-walled steel beams. In current design codes, the capacity prediction for LT buckling is typically realized by using the critical moment, hence, the accurate calculation of the critical moment is essential.

Lateral-torsional buckling is a global phenomenon, in which the cross-section deformations are negligibly small. When the member buckles in LTB, the buckled shape is the combination of flexural displacement in the lateral direction and twisting displacement along the member axis. The classic description of the problem and the solution for some basics cases are presented in many textbooks (Vlasov, 1961). Though the underlying differential equation (D.E.) is known, except some simplest cases, the exact analytical solution of the D.E. is difficult to find.

[1] PhD student, Budapest University of Technology and Economics, <hoang.trung@epito.bme.hu>
[2] Professor, Budapest University of Technology and Economics, <adany.sandor@epito.bme.hu>

Beams are frequently supplemented by transverse plate elements. Such transverse plate may appear as an end-plate, a gusset plate, or a transverse stiffener. End-plates and gusset plates are applied in order to facilitate the connection between the various structural members (i.e., a beam to a column), while stiffeners are typically applied in order to increase the resistance to the buckling of slender plates. Though stiffeners, end-plates and gusset plates have different roles, they might have different shapes, etc., they have very similar mechanical effects on the torsional and flexural behavior of members. Thus, the term "transverse stiffener" will be used in this paper, but in a general meaning.

Transverse stiffeners are well-known to be effective against shear buckling of a web or against web crippling at supports, but their effect on the global buckling got little attention so far. In Hoang and Ádány (2020a) and Hoang and Ádány (2020b) the pure torsional buckling of I-section columns with stiffeners has recently been investigated. Though pure torsional buckling is a relatively unique phenomenon, its solution paved the way toward lateral-torsional buckling, which is practically much more important, and which is the topic of this actual paper.

According to the authors' best knowledge, an analytical solution for lateral torsional buckling of thin-walled beams with directly considering transverse stiffeners or end-plates is not yet reported. This gap is intended to fill here, where analytical solutions for the critical load to lateral torsional buckling of thin-walled beams with transverse elements is presented. The analytical solutions are validated by comparing the analytical results to those from shell finite element solutions. For shell FE the commercial finite element software Ansys (Ansys, 2019), as well as the special constrained finite element method (cFEM) is used, see Ádány (2018b) and Ádány et al. (2018). More precisely, cFEM has recently been extended to members with transverse plate elements (Hoang and Ádány (2020c), which cFEM version is employed here.

In the paper, first the analytical derivation is summarized for doubly-symmetric I-section beams in Section 2. Then the cFEM is briefly introduced in Section 3. In Section 4 numerical results are presented for various problems. Finally, the main conclusions are summarized.

2. Analytical solution: I-section beams with rectangular stiffeners

2.1 General

In this Section the analytical solution for lateral torsional buckling is derived for a doubly-symmetrical I-section member stiffened by rectangular plates. The main assumptions and the steps of the derivation are identical those for pure torsional buckling, presented in Hoang and Ádány (2020a) and Hoang and Ádány (2020b), summarized as follows.

As Fig. 1 illustrates, the depth and width of the member cross-section is h and b, respectively, interpreted as midline dimensions. The member length is L. The member is subjected to uniform moment, i.e., two concentrated end moments are considered as loading.

The stiffeners are kept symmetric with respect to the web position and also perpendicular to the member axis. In a general case n_{st} transverse plates are considered, the position of each is given by $x_{st,i}$ $(i = 1, \dots, n_{st,} 0 \leq x_{st,i} \leq L)$. The i-th stiffener plate has a thickness $t_{st,i}$, its height and width are $h_{st,i}$ and $b_{st,i}$, respectively, and it is assumed that $h_{st,i} \leq h$ and $b_{st,i} \leq b$. The coordinate system defined in such a manner that its O origin would coincide the C centroid of the cross section, which is also the shear center.

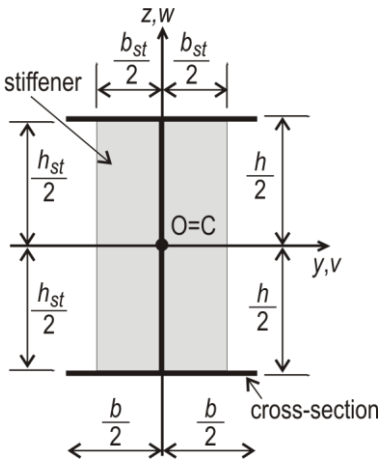

Figure 1: I-section with transverse stiffeners: notations, coordinates, dimensions

The member is modeled as a one-dimensional element with cross-sections perpendicular to the member axis, i.e., beam-model is adopted. The cross-sections are assumed to be rigid, hence the displacement of the member can be expressed by the displacement function of the member axis. Classic beam theory is assumed, that is for the torsional behavior Vlasov's theory is applied (which can be regarded as the extension of the classic Euler-Bernoulli beam theory). The material is linearly elastic, isotropic. Since the immediate goal here is to solve the linear buckling problem for lateral-torsional buckling, the displacement of the member is described by the functions of the twisting rotation $\theta(x)$ and the lateral translation $v(x)$ (while the flexural displacement in the plane of the bending is not needed). The assumed displacement functions have to satisfy the boundary conditions defined by the supports. Two types of supports will be considered here, and the displacement functions will be assumed accordingly, see Section 2.2 and Section 2.3, respectively.

The stiffeners are assumed to be thin plates, hence the $w_{st,i}(y,z)$ displacement function of the i-th stiffener (where $i = 1,\dots,n_{st}$) should satisfy the differential equation (D.E.) of the Kirchhoff-Love plate theory, plus it should satisfy the boundary conditions, too. The boundary conditions of the stiffeners partly come from the compatibility between the member and the stiffener, and partly come from the static conditions at the free edges of the plates. The D.E. of the plate is as follows:

$$\Delta\Delta w_{st,i}(y,z) = \frac{\partial^4 w_{st,i}}{\partial y^4} + 2\frac{\partial^4 w_{st,i}}{\partial y^2 \partial z^2} + \frac{\partial^4 w_{st,i}}{\partial z^4} = \frac{p_{st,i}}{D_{st,i}} \tag{1}$$

where $D_{st,i} = \frac{E{t_{st,i}}^3}{12(1-\nu^2)}$, is the plate stiffness and $t_{st,i}$ is thickness of stiffener, E is modulus of elasticity, ν is Poisson's ratio, while $p_{st,i}$ is the load acting perpendicularly on the plate. In the actual problem this load is zero, hence the right-hand-side of the D.E. is zero.

The analytical solution is based on the energy method: the total potential is expressed by some displacement parameters, then the theorem of stationarity of potential energy is used to find the equilibrium configuration. As far as the main member is concerned, the classic energy/work terms are applied. This means that the methodology followed here leads to the classic critical moment formula for lateral-torsional buckling if no transverse stiffeners are added. However, here the effect of the stiffeners is also considered. This effect is two-fold: (i) the transverse stiffeners contribute to the strain energy (hence the total potential), and (ii) the transverse stiffeners have influence on the longitudinal distribution of the displacements. The derivations will briefly be presented for two cases. In Section 2.2 only the first effect is considered (by assuming that the second effect is negligible), while in Section 2.3 both effects are directly considered.

2.2 Clamped-clamped beam

In this Section the solution for a clamped-clamped beam member with n_{st} identical stiffeners is presented. For the sake of simplicity, the stiffeners are assumed to be evenly distributed along the length, i.e., in the case of one single stiffener it is at mid-length, in the case of two stiffeners they are at the third-points, etc.

For this case, the assumed longitudinal displacement functions are:

$$\theta = \theta_0 \frac{1}{2}\left[1 - \cos\left(\frac{2\pi x}{L}\right)\right] \tag{2}$$

$$v = v_0 \frac{1}{2}\left[1 - \cos\left(\frac{2\pi x}{L}\right)\right] \tag{3}$$

These functions are frequently used for clamped-clamped columns or beams (without stiffeners), however, it is good to know that for the lateral-torsional buckling of beams these functions are approximate even without stiffeners. The numerical results suggest however, (see Section 4,) that they are applicable with reasonable precision if the stiffeners are not too strong.

The external potential is the negative of the work done by the loading on the second-order displacements. Since the only assumed loading is pure bending, the external potential is calculated from the work of the end moments (M_y) on the rotation of the end cross-sections ($\emptyset_y$). Mathematically:

$$\Pi_{ext} = -2M_y\emptyset_y = -M_y \frac{(\Delta_{x,bottom} - \Delta_{x,top})}{h} \tag{4}$$

where M_y is external bending moment acting on the member, h is the height of the cross section, and $\Delta_{x,bottom}$ and $\Delta_{x,top}$ are the elongations of the top and bottom fibers of the cross-section at the junction points of the web and flanges. The total elongation of the fiber can be calculated from the longitudinal second-order strain terms, as follow:

$$\Delta_x = \int_0^L \varepsilon_x^{II} dx = \int_0^L \frac{1}{2}\left(\left(\frac{\partial v_{loc}}{\partial x}\right)^2 + \left(\frac{\partial w_{loc}}{\partial x}\right)^2\right) dx \tag{5}$$

By applying the above formula to the top and bottom fibres:

$$\Delta_{x,bottom} = \int_0^L \frac{1}{2}\left(\left(\frac{\partial v_{loc,b}}{\partial x}\right)^2 + \left(\frac{\partial w_{loc,b}}{\partial x}\right)^2\right) dx \tag{6}$$

$$\Delta_{x,top} = \int_0^L \frac{1}{2}\left(\left(\frac{\partial v_{loc,t}}{\partial x}\right)^2 + \left(\frac{\partial w_{loc,t}}{\partial x}\right)^2\right) dx \tag{7}$$

where:

$$v_{loc,b} = v + \theta h/2 \text{ and } w_{loc,b} = 0 \tag{8}$$

$$v_{loc,t} = v - \theta h/2 \text{ and } w_{loc,t} = 0 \tag{9}$$

Substituting Eqs. (6-9) into Eq. (4), the external potential can finally be expressed as:

$$\Pi_{ext} = -M_y \frac{v_0 \theta_0 \pi}{2L} \tag{10}$$

The internal potential is the accumulated strain energy. The strain energy in the main member is due to bending in *y-z* plane, due to Saint-Venant torsion, and due strains and stresses associated with warping. Without showing the details of the derivations, we got the following energy terms for the above three components:

$$\Pi_{int}^{b} = \frac{1}{2}\int_0^L EI_z \left(\frac{\partial^2 v}{\partial x^2}\right)^2 \mathrm{d}x = EI_z \frac{\pi^3}{12L^3}(12\pi {v_0}^2) \tag{11}$$

$$\Pi_{int}^{S-V} = \frac{1}{2}\int_0^L GI_t \left(\frac{\partial \theta}{\partial x}\right)^2 \mathrm{d}x = GI_t \frac{\pi}{12L}\left(3\pi {\theta_0}^2\right) \tag{12}$$

$$\Pi_{int}^{warp} = \frac{1}{2}\int_0^L EI_\omega \left(\frac{\partial^2\theta}{\partial x^2}\right)^2 \mathrm{d}x = EI_\omega \frac{\pi^3}{12L^3}\left(12\pi{\theta_0}^2\right) \tag{13}$$

where I_z is the moment of inertial about *z*-axis, I_t is the torsional constant, I_ω is the warping constant, *E* is the modulus of elasticity, *G* is the shear modulus.

The strain energy in a stiffener plate can be calculated from the curvatures and stress resultants (i.e., moments). The detailed derivations can be seen in Hoang and Ádány (2020b). The solution can be summarized with the equation as follows:

$$\Pi_{int,i}^{st} = (\theta'_{si})^2 D_{st,i} C_{st,i} \tag{14}$$

where $D_{st,i}$ is the plate stiffness, given by Eq. (1), and θ'_{si} is the derivative of the twisting function at the position of the *i*-th stiffener. The coefficient $C_{st,i}$ is dependent on how the stiffener plate is connected to the main member. Here we consider three cases: (a) the stiffener is connected to the flanges only, (b) the stiffener is connected to the web only, and (c) the stiffener is connected to the web and flanges. It is the third connection type which is typically applied in the practice, however the first two (slightly theoretical) cases is considered, too, in order to better understand the role of the stiffener-to-member connection on the buckling behavior. The $C_{st,i}$ coefficients are expressed for the three cases, respectively, as follows:

$$C_{st,i}{}^{(a)} = \frac{b_{st,i}\left(10{b_{st,i}}^2 - 9{h_{st,i}}^2\nu + 9{h_{st,i}}^2\right)}{5h_{st,i}} \tag{15}$$

$$C_{st,i}{}^{(b)} = {h_{st,i}}^2 \left[\frac{b_{st,i}}{2bst_i}(c_i - 1)^2 - \frac{b_{st,i}}{5h_{st,i}}(1-\nu)(-6{c_i}^2 + 2c_i - 1)\right], \tag{16}$$

with:

$$c_i = \frac{4\cdot G\cdot {b_{st,i}}^2 + 5\cdot E\cdot {h_{st,i}}^2}{24\cdot G\cdot {b_{st,i}}^2 + 5\cdot E\cdot {h_{st,i}}^2}, \tag{17}$$

$$C_{st,i}{}^{(c)} = \frac{b_{st,i}\left(10{b_{st,i}}^2 - 9{h_{st,i}}^2\nu + 9{h_{st,i}}^2\right)}{5hst_i} + \frac{8}{525}\frac{30{\bar{b}_{st,i}}^4 + 14{\bar{b}_{st,i}}^2{h_{st,i}}^2 + 5{h_{st,i}}^4}{\bar{b}_{st,i}h_{st,i}}, \tag{18}$$

with $\bar{b}_{st,i} = kb_{st,i}$, where *k* is a parameter (between 0 and 1) the proper value of which is dependent on various parameters of the problem.

It is to mention that while in the "flanges-only" and "web-only" cases the above expressions are exact (in the sense that they satisfy all the considered conditions), in the case of "web-and-flanges" connection there is no exact solution for the plate displacement and the above expression is approximate only.

To obtain the strain energy of the member, we need to summarize all the above energy terms:

$$\Pi_{int} = \Pi_{int}^{b} + \Pi_{int}^{S-V} + \Pi_{int}^{warp} + \sum_1^{n_{st}} \Pi_{int,i}^{st} \tag{19}$$

The total potential of the whole member is:

$$\Pi = \Pi_{int} + \Pi_{ext} = EI_z \frac{\pi^3}{12L^3}(12\pi{v_0}^2) + GI_t \frac{\pi}{12L} 3\pi{\theta_0}^2 + EI_\omega \frac{\pi^3}{12L^3} 12\pi{\theta_0}^2 + \frac{\pi^2}{L^2}{\theta_0}^2 D_{st,i} C_{st,i} \sum_1^{n_{st}} \sin^2\left(\frac{2\pi}{L}x_{st,i}\right) - M_y \frac{v_0\theta_0\pi}{2L} \tag{20}$$

In equilibrium the total potential is stationary, which leads to a following system of equations:

$$\frac{\partial\Pi}{\partial\theta_0} = GI_t \frac{\pi}{2L}\pi\theta_0 + EI_\omega \frac{\pi^3}{L^3} 2\pi\theta_0 + D_{st,i}C_{st,i}\frac{\pi^2}{L^2} 2\theta_0 \sum_1^{n_{st}} \sin^2\left(\frac{2\pi}{L}x_{st,i}\right) - M_y \frac{v_0\pi}{2L} = 0 \tag{21}$$

$$\frac{\partial\Pi}{\partial v_0} = EI_z \frac{\pi^3}{L^3}(2\pi v_0) - M_y \frac{\theta_0\pi}{2L} = 0 \tag{22}$$

This system of equations can be summarized in the matrix form as follow:

$$\begin{bmatrix} F_{cr,z} & -M_y \\ -M_y & {r_0}^2 F_{cr,\theta} \end{bmatrix} \begin{bmatrix} v_0 \\ \theta_0 \end{bmatrix} = \begin{bmatrix} 0 \\ 0 \end{bmatrix} \tag{23}$$

where:

$$F_{cr,\theta} = \frac{1}{{r_0}^2}\left(GI_t + 4EI_\omega \frac{\pi^2}{L^2} + \frac{4}{L} D_{st} C_{st} \sum_1^{n_{st}} \sin^2\left(\frac{2\pi}{L} x_{st,i}\right)\right) \tag{24}$$

$$F_{cr,z} = 4EI_z \frac{\pi^2}{L^2} \tag{25}$$

Note, if the shear center of the main member cross section coincides with the origin of the coordinate system, (which is the case now,) then

$$\int_A \frac{\left(z^2+y^2\right)}{A} dA = {r_0}^2 \tag{26}$$

which is the polar radius of gyration of the cross-section.

Eq. (23) has non-trivial solution if the coefficient matrix is singular, therefore:

$${r_0}^2 F_{cr,\theta} F_{cr,z} - M_y^2 = 0 \tag{27}$$

from which the value of the critical bending moment can be expressed:

$$M_{cr,y} = \pm\sqrt{4EI_z \frac{\pi^2}{L^2}\left(GI_t + 4EI_\omega \frac{\pi^2}{L^2} + \frac{4}{L} D_{st} C_{st} \sum_1^{n_{st}} \sin^2\left(\frac{2\pi}{L} x_{st,i}\right)\right)} \tag{28}$$

$$M_{cr,y} = \pm r_0 \sqrt{F_{cr,\theta} F_{cr,z}} \tag{29}$$

It can be seen that Eq. (29) is formally identical to the classic solution for beams without stiffeners, however, $F_{cr,\theta}$ (i.e., the critical force to pure torsional buckling) includes the effect of the stiffeners. It is to mention that $F_{cr,\theta}$, as in Eq. (24), is indeed identical to the critical force to pure torsional buckling of I-members with stiffeners, see Hoang and Ádány (2020b). It is interesting to observe that the influence of the stiffener appears as an additional term (beside the Saint-Venant and warping terms) in the critical force formula. It can also be understood that the effect of the stiffeners is dependent on various factors, including the plate size and thickness, the number and the positions of the stiffener plates, and also on how the stiffener plate is connected to the main member.

2.3 Pinned-pinned beam with end-plates

In this Section the solution for a member with pinned-pinned supports and with end-plates is presented. Thus, there are two stiffeners, at $x_1 = 0$ and $x_2 = L$, and the two end-plates are identical. It is reasonable to assume that the effect of the end-plates is negligible on the flexural behavior, hence the classical half sine-wave can be assumed for the lateral translation function. However, end-plates can have significant effect on the twisting behavior of the member, since the end-plate, if sufficiently rigid, means some restraint against warping. If the end-plates are very thin, then the behavior of the beam will be nearly identical to that of a pinned-pinned beam without stiffeners; in this case a half sine-wave function is reasonable to consider for the twisting rotation function. If the end-plates are very thick, then the twisting behavior of the member will be similar to the case of a clamped-clamped support; the twisting rotation function can be assumed as in Eq. (2). In a general case, therefore, the twisting displacement function can be assumed as the linear combination of these two functions. Therefore, the assumed displacement functions are as follow:

$$\theta = \theta_{0,1} \sin\left(\frac{\pi x}{L}\right) + \theta_{0,2} \frac{1}{2}\left[1 - \cos\left(\frac{2\pi x}{L}\right)\right] \tag{30}$$

$$v = v_0 \sin\left(\frac{\pi x}{L}\right) \tag{31}$$

The same calculation process can be repeated as presented previously in Section 2.2. The total potential energy function is expressed by two displacement parameters $\theta_{0,1}$ and $\theta_{0,2}$, as follows.

$$\Pi = EI_z \frac{\pi^3}{12L^3}(3\pi {v_0}^2) + GI_t \frac{\pi}{12L}\left(3\pi {\theta_{0,1}}^2 + 16\theta_{0,1}\theta_{0,2} + 3\pi {\theta_{0,2}}^2\right) + EI_\omega \frac{\pi^3}{12L^3}\left(3\pi {\theta_{0,1}}^2 + 16\theta_{0,1}\theta_{0,2} + 12\pi {\theta_{0,2}}^2\right) + +2\frac{\pi^2}{L^2}{\theta_{0,1}}^2 D_{st} C_{st} - M_y \frac{v_0(3\pi\theta_{0,1} + 8\theta_{0,2})\pi}{6L} \tag{32}$$

In equilibrium the total potential is stationary, which leads to a following equation:

$$\begin{bmatrix} 3\pi EI_z \frac{\pi^2}{L^2} & -3\pi M_y & -8M_y \\ -3\pi M_y & 3\pi\left(GI_t + EI_\omega \frac{\pi^2}{L^2} + \frac{8D_{st}C_{st}}{L}\right) & 8\left(GI_t + EI_\omega \frac{\pi^2}{L^2}\right) \\ -8M_y & 8\left(GI_t + EI_\omega \frac{\pi^2}{L^2}\right) & 3\pi\left(GI_t + 4EI_\omega \frac{\pi^2}{L^2}\right) \end{bmatrix} \begin{bmatrix} v_0 \\ \theta_{0,1} \\ \theta_{0,2} \end{bmatrix} = \begin{bmatrix} 0 \\ 0 \\ 0 \end{bmatrix} \tag{33}$$

It is to observe that the above equation can also be written as:

$$\begin{bmatrix} F_{cr,z} & -3\pi M_y & -\frac{8}{3\pi} M_y \\ -M_y & {r_0}^2 F_1 & \frac{8}{3\pi} {r_0}^2 F_{12} \\ -\frac{8}{3\pi} M_y & \frac{8}{3\pi} {r_0}^2 F_{12} & {r_0}^2 F_2 \end{bmatrix} \begin{bmatrix} v_0 \\ \theta_{0,1} \\ \theta_{0,2} \end{bmatrix} = \begin{bmatrix} 0 \\ 0 \\ 0 \end{bmatrix} \tag{34}$$

where F_1 is the critical force to pure torsional buckling of the same member (if subjected to axial force) with considering a displacement function $\theta_1 = \theta_{0,1} \sin\left(\frac{\pi x}{L}\right)$, and F_2 and F_{12} are the critical forces to the same member but without stiffeners for clamped-clamped support and pinned-pinned support, respectively.

From the above generalized eigen-value problem the critical bending moment can be obtained. The determinant of the coefficient matrix leads to the following quadratic equation for M_y:

$${M_y}^2\left(F_2 + \frac{64}{9\pi^2}F_1 - \frac{128}{9\pi^2}F_{12}\right) - {r_0}^2 F_{cr,z}\left(F_1 F_2 - \frac{64}{9\pi^2}{F_{12}}^2\right) = 0 \tag{35}$$

From the above equation the value of the critical bending moment is as follows:

$$M_{cr,y} = \pm r_0 \sqrt{\frac{\left(F_1 F_2 - \frac{64}{9\pi^2}{F_{12}}^2\right) F_{cr,z}}{\left(F_2 + \frac{64}{9\pi^2}F_1 - \frac{128}{9\pi^2}F_{12}\right)}} \tag{36}$$

It can be noticed that the above expression is different even formally from Eq. (29), though the involved terms are similar.

3. Constrained finite element method for members with transverse plates

In order to validate the derived analytical formulae, numerical examples are solved (see Section 4), and the obtained analytical results are compared to those from numerical methods, namely a shell finite element method. A specific numerical method is also used: the constrained finite element method (cFEM). This is essentially a shell finite element method, but with an ability to perform modal decomposition, e.g. to analyze a thin-walled beam or column member by constraining the displacements into predefined, practically meaningful mode types. The method was presented in several papers, see e.g. Ádány (2018b) and Ádány et al. (2018). Recently, cFEM has been extended to members with transverse plate elements, too, as reported in detail in Hoang

and Ádány (2020c). This specific version of cFEM will be applied here. Since we want to analyse lateral-torsional buckling, which is a global type of buckling, in the application of cFEM the displacements will be constrained into global modes. It is to mention, however, that the constraints are applied to the main member only, which means that the stiffeners can freely deform.

Since one of the important effects of the stiffener is that they modify the longitudinal distribution of the displacements (with respect to the one of a similar member but without stiffeners), the cFEM will be employed to numerically analyze this effect. For this reason, cFEM will be applied in two options.

When the classic cFEM is employed, the displacement functions are expressed as the linear combination of shape functions. The shape functions are (mostly) cubic, so-called Hermite polynomials. For example, both the lateral translation and the twisting rotation function is expressed as:

$$f(x) = \sum_i \emptyset_i c_i \tag{36}$$

where $\emptyset_i$ denotes the shape functions, and c_i are the combination factors (which, in the case of global modes, have the physical meaning of "cross-section displacements"). This is illustrated in Fig. 2.

It is obvious that the linear combination of the cubic shape functions does not enforce the member to deform as assumed in the analytical solution, see Eqs. (2-3) and Eqs. (30-31). However, in the cFEM it is relatively straightforward to consider other shape functions, too. This feature of cFEM has been utilized e.g. in Ádány (2018a) to create the so-called generalized signature curves, and this is the feature which is used in Ádány (2019) for mode identification. In this paper, therefore, we will use cFEM by enforcing the displacement functions to be identical to those assumed in the analytical solutions. Instead of having multiple cubic functions, we use one or two trigonometric shape functions only, as illustrated in Fig. 3. This special version of cFEM will be referred to as "cFEM enforced", while the classic cFEM will simply be referred to as "cFEM".

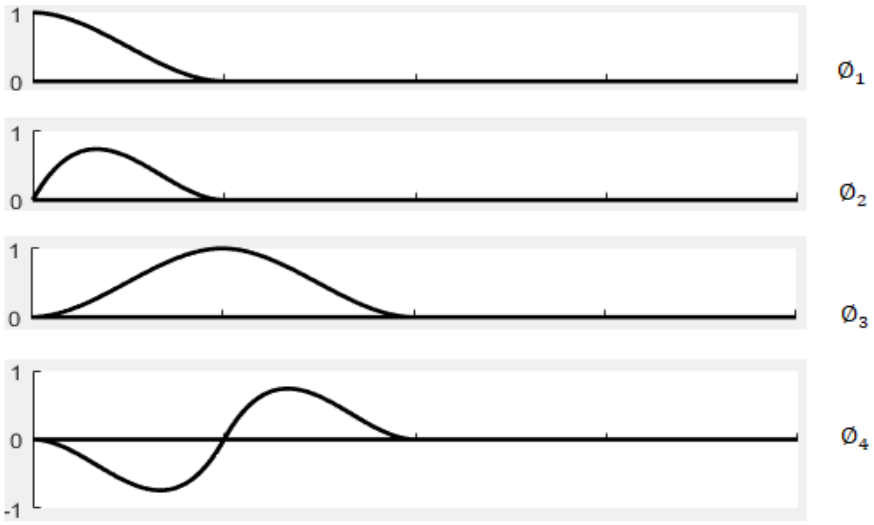

Figure 2: Demonstration of shape functions in the longitudinal direction in classic cFEM

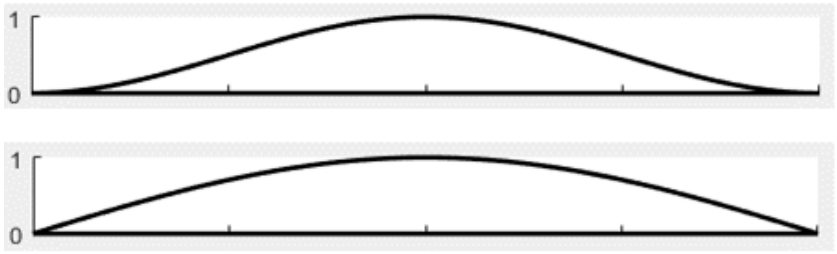

Figure 3: Demonstration of global shape functions in "cFEM enforced"

4. Numerical examples

Two sets of numerical examples are presented. The critical buckling loads are calculated using the analytical formulae presented in Section 2. Then, the results are compared to those from constrained finite element method and from ANSYS shell finite element analyses. In ANSYS, Shell181 elements are adopted. The mesh size of the shell elements was kept approx. 50 mm in both the cFEM and the ANSYS model.

4.1 Example: clamped-clamped beam with multiple stiffeners

In this example a clamped-clamped I-section member is studied with multiple stiffeners. The stiffeners are equally spaced along the member length, i.e., in the case of one single stiffener it is at mid-length, in the case of two stiffeners they are at the third-points, etc. In the shell models the clamped-clamped support is implemented in such a manner that it prevents rotations and transverse translations only, but the longitudinal translation at the supports is allowed. The cross-section is similar to an IPE300 hot-rolled steel profile. More specifically the cross-section depth is h=300 mm, the width is b=150 mm, the flange thickness is t_f=10.7 mm, the web thickness is t_w=7.1 mm. (The depth and width values are interpreted for the midline of the cross-section.) The material is isotropic linearly elastic steel, with E=210000 MPa and ν=0.3.

The stiffener width and height is equal to the width and depth of the cross-section. The t_{st} stiffener thickness varies between $0.5t_w$ and $5t_w$. Its material is identical to that of the main member. The loading is two concentrated bending moments about the y axis, identical in magnitude but opposite in direction, applied at the member ends. The concentrated bending moments are placed onto the shell model as line loads, distributed along the cross-section mid-line.

The analyses are performed for two different lengths, 6 m and 8 m, and the results of analytical results are compared to the cFEM results. In the case of the cFEM, the results are calculated in two options: by using the classic cFEM shape functions, or by using the shape functions in accordance with the assumption of the analytical solution. These two options are referred to as "cFEM" and "cFEM enforced", respectively. Furthermore, the results are calculated by considering three stiffener-to-member connections: "flanges-only", web-only", and "web-and-flanges".

In Figure 4 the critical bending moment is plotted for selected parameters and options. All the curves show linearly increasing tendencies as the number of stiffeners are increasing (at least if the number of stiffeners is larger than one). This linear tendency indeed can be proved mathematically by the analytical formulae. The same tendency is clearly observable from the cFEM results, too. The analytical results and the "cFEM enforced" results are practically identical, while the results from the classic cFEM are systematically smaller. Though the difference is not

large, this discrepancy demonstrates that the assumed simple trigonometric displacement function is not entirely precise, especially not if stiffeners are present.

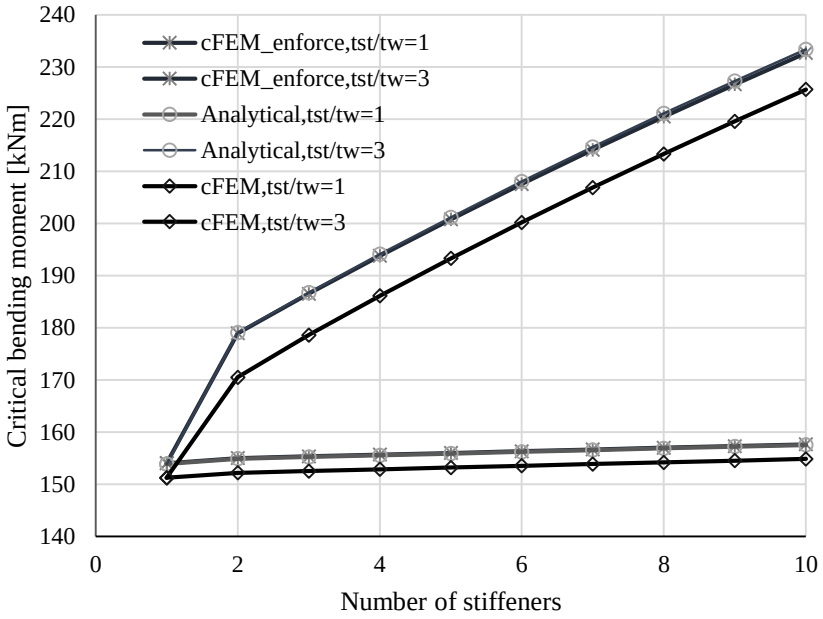

Figure 4: Critical bending moment in the function of the number of stiffeners, L=8m

Tables 1 and 2 summarize how the critical moment is increased due to the presence of the stiffeners, depending on the member length, and depending on the stiffener-to-member connection. The results show very good agreement between the cFEM, in which the enforced option was used, and the analytical solutions in the "Flanges-only" and "Web-only" cases for both lengths and for various stiffener thickness values, while discrepancy between the cFEM and the analytical solutions can be observed in the "Web-and-flanges" cases. This observation can be explained by the important fact that the displacement function of the stiffener plate, which is used in the derivation of the analytical solution, is only an approximation. It is expected that the differences are bigger in these cases. From the analysis results it is clear that the connection of the stiffener to the flanges of the member has more influence compared to the connection to the web. As it can be seen in Tables 1 and 2, the critical bending moment increments due to the connection to the flanges is approx. 3-3.5 times larger than the increments due to the connection to the web.

The appearance of the stiffeners has two effects on the critical load of the member. The direct effect comes from the stiffness of each individual stiffener, which add extra energy terms to the strain energy. The other, indirect effect comes from the modification of the longitudinal distribution of the displacements. This latter effect can be studied from Table 3, since this latter effect is the one that causes the differences between the "cFEM" and "cFEM enforced" results. As clear from Table 3, the "cFEM enforced" and the analytical results are nearly identical, while there is a more significant difference between the "cFEM and the "Analytical" results. It can also be observed that this secondary effect of the stiffeners is smaller and smaller as the number of stiffeners is increasing, which is clear from Fig. 5, too.

Table1: Critical bending moment increments due to multiple stiffeners, L=6m

	Number of stiffeners	*tst=tw*				*tst=2tw*			
		Flange only[1] (kNm)	Web only[2] (kNm)	Full[3] (kNm)	Flange contr.[4]	Flange only (kNm)	Web only (kNm)	Full (kNm)	Flange cont.
cFEM	1	0.00	0.00	0.00	0%	0.00	0.00	0.00	0%
	2	1.54	0.43	1.73	89.2%	11.49	3.43	13.49	85.1%
	3	2.02	0.58	2.30	88.0%	15.18	4.57	17.83	85.1%
	4	2.50	0.72	2.87	87.2%	18.82	5.70	22.11	85.1%
	5	2.99	0.86	3.44	86.7%	22.40	6.82	26.31	85.1%
	6	3.47	1.01	4.01	86.4%	25.95	7.94	30.46	85.2%
	7	3.94	1.15	4.58	86.2%	29.44	9.05	34.54	85.2%
	8	4.42	1.29	5.15	86.0%	32.90	10.16	38.56	85.3%
	9	4.90	1.44	5.71	85.8%	36.31	11.27	42.53	85.4%
	10	5.38	1.58	6.27	85.7%	39.68	12.37	46.45	85.4%
Analytical	1	0.00	0.00	0.00	0%	0.00	0.00	0.00	0%
	2	1.49	0.45	2.13	69.7%	11.66	3.56	16.05	72.6%
	3	1.98	0.60	2.81	70.4%	15.44	4.74	21.17	72.9%
	4	2.47	0.75	3.49	70.9%	19.15	5.91	26.18	73.2%
	5	2.97	0.90	4.17	71.2%	22.82	7.08	31.11	73.4%
	6	3.46	1.04	4.84	71.4%	26.44	8.24	35.95	73.5%
	7	3.95	1.19	5.52	71.6%	30.01	9.40	40.71	73.7%
	8	4.44	1.34	6.19	71.7%	33.54	10.55	45.39	73.9%
	9	4.93	1.49	6.86	71.8%	37.02	11.69	50.00	74.0%
	10	5.41	1.64	7.53	71.9%	40.46	12.83	54.54	74.2%

[1] Only the flanges of the main member are connected to the stiffeners.
[2] Only the web of the main member is connected to the stiffeners.
[3] Both the flanges and web of the main member are connected to the stiffeners
[4] The percentage contribution to the critical moment increment of the stiffeners of the stiffeners-flanges connection.

Table 2: Critical bending moment increments due to multiple stiffeners, *L*=8m

	Number of stiffeners	*tst=tw*				*tst=2tw*			
		Flange only[1] (kNm)	Web only[2] (kNm)	Full [3] (kNm)	Flange contr.[4]	Flange only (kNm)	Web only (kNm)	Full (kNm)	Flange cont.
cFEM	1	0.00	0.00	0.00	0%	0.00	0.00	0.00	0%
	2	1.05	0.29	1.18	88.8%	7.85	2.32	9.22	85.2%
	3	1.38	0.39	1.58	87.7%	10.37	3.09	12.17	85.2%
	4	1.71	0.49	1.97	87.0%	12.85	3.86	15.08	85.2%
	5	2.04	0.59	2.36	86.6%	15.29	4.62	17.94	85.2%
	6	2.37	0.68	2.75	86.3%	17.70	5.37	20.75	85.3%
	7	2.70	0.78	3.14	86.0%	20.08	6.12	23.52	85.4%
	8	3.03	0.88	3.52	85.9%	22.42	6.87	26.24	85.4%
	9	3.35	0.97	3.91	85.8%	24.73	7.62	28.92	85.5%
	10	3.68	1.07	4.29	85.6%	27.01	8.36	31.57	85.6%
Analytical	1	0.00	0.00	0.00	0%	0.00	0.00	0.00	0%
	2	1.01	0.30	1.43	70.4%	7.88	2.41	10.83	72.8%
	3	1.34	0.40	1.89	70.9%	10.43	3.21	14.27	73.0%
	4	1.68	0.51	2.35	71.3%	12.93	4.00	17.65	73.3%
	5	2.01	0.61	2.81	71.5%	15.40	4.79	20.96	73.5%
	6	2.34	0.71	3.26	71.7%	17.83	5.57	24.21	73.7%
	7	2.67	0.81	3.72	71.8%	20.23	6.35	27.39	73.9%
	8	3.00	0.91	4.17	71.9%	22.60	7.13	30.53	74.0%
	9	3.33	1.01	4.63	72.0%	24.93	7.90	33.61	74.2%
	10	3.66	1.11	5.08	72.1%	27.24	8.67	36.64	74.3%

[1] Only the flanges of the main member are connected to the stiffeners.
[2] Only the web of the main member is connected to the stiffeners.
[3] Both the flanges and web of the main member are connected to the stiffeners
[4] The percentage contribution to the critical moment increment of the stiffeners of the stiffeners-flanges connection.

Table3: Critical bending moment of IPE300 with multiple stiffeners, *L*=6m, *tst/tw=5*

No. stiffeners	cFEM enforced		cFEM		Analytical		Differences			
	Flange only (kNm)	Web only (kNm)	Flange only (kNm)	Web only (kNm)	Flange only (kNm)	Web only (kNm)	cFEM enforced vs. Ana		cFEM vs. Ana	
							Flange-only	Web-only	Flange-only	Web-only
1	247.23	247.23	242.54	242.54	247.06	247.06	0.07%	0.07%	1.83%	1.83%
2	388.37	296.2	318.83	280.18	391.42	297.92	0.78%	0.58%	18.55%	5.95%
3	425.12	310.82	359.37	296.1	428.87	313.05	0.88%	0.71%	16.21%	5.41%
4	458.93	324.78	395.45	310.66	463.31	327.47	0.95%	0.82%	14.65%	5.13%
5	490.41	338.16	428.86	324.44	495.36	341.29	1.00%	0.92%	13.42%	4.94%
6	519.99	351.03	460.18	337.62	525.45	354.57	1.04%	1.00%	12.42%	4.78%
7	547.98	363.45	489.76	350.29	553.92	367.37	1.07%	1.07%	11.58%	4.65%
8	574.61	375.46	517.83	362.50	580.99	379.74	1.10%	1.13%	10.87%	4.54%
9	600.05	387.09	544.59	374.31	606.85	391.71	1.12%	1.18%	10.26%	4.44%
10	624.46	398.39	570.21	385.76	631.66	403.34	1.14%	1.23%	9.73%	4.36%

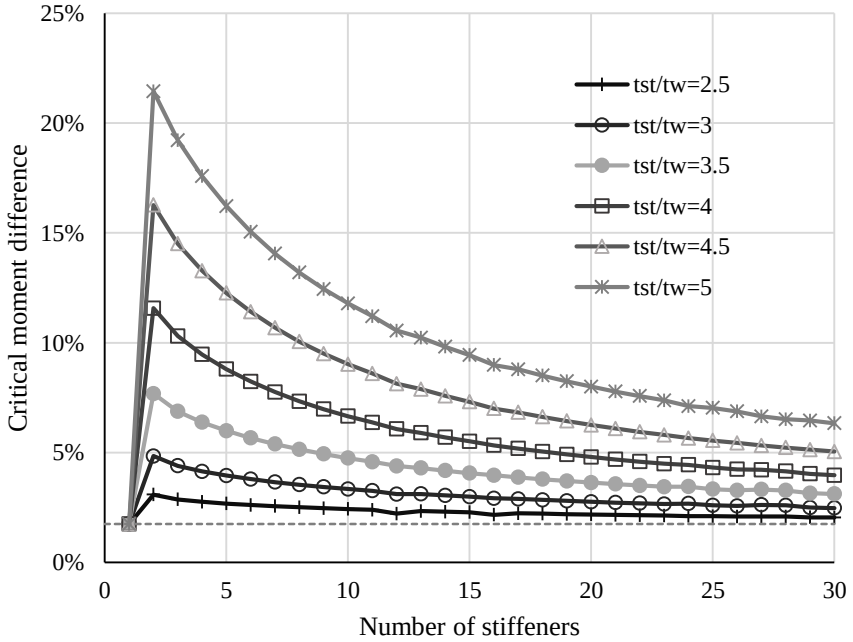

Figure 5: Critical bending moment difference between cFEM and Analytical in the function of the number of stiffeners, *L*=8 m

4.2 Example: pinned-pinned beam with end-plates

In this example pined-pined I-section beams with end-plates are studied. The material is the same as in the previous examples. The analysis is performed for two different cross-sections, an IPE300-like and a HEA300-like one. For the IPE300-like cross-section the cross-section dimensions are

identical with those described in the previous Section. In the case of HEA300 the depth is h=300 mm, the width is b=300mm, the flange thickness is t_f=20.5 mm, and the web thickness is t_w=11.5. Two different member lengths, 6m and 8m, are analyzed with the t_{st}/t_w ratio varying between 0.5 and 10. The analytical results are then compared to those from finite element solutions, both cFEM and ANSYS.

The results are summarized in the plots of Figs. 6 and 7. In both plots the critical moments are shown (for two member lengths) in the function of the end-plate thickness. For both sections the tendencies are similar, and the results are in accordance with the engineering expectations. With the increase of the end-plate thickness, the critical moments are increasing and converging to a plateau. The larger and larger critical values are due to the larger and larger warping restraint, which gradually transforms the longitudinal distribution of the twisting function from the half sine-wave to the cosine function, as can be observed in Fig. 8.

Though the above-described tendency is characteristic to all the 4 considered options, the differences between the various options is visible, too. As far as the options are concerned, it can be observed that: the more constrained the method is, the higher the critical load is. In the case of Ansys calculations there is no extra constraint beside the end supports, which means that small localized plate-like deformations, as well as shear deformations of the plate elements are allowed to occur and do occur. When cFEM is used, these deformations are excluded, but the member axis can freely deform between the supports. In the case of "cFEM enforced" options and the analytical solutions the longitudinal displacements are further constrained according to the predefined trigonometric functions. Finally, though the difference between the "cFEM enforced" and the "Analytical" results is fairly small, still, it is the "Analytical" that predicts systematically larger critical values. This small difference is due to the fact that even though the displacements of the main member are practically identical in the "cFEM enforced" and the "Analytical" options, the deformations of the stiffeners are slightly less restricted in the cFEM.

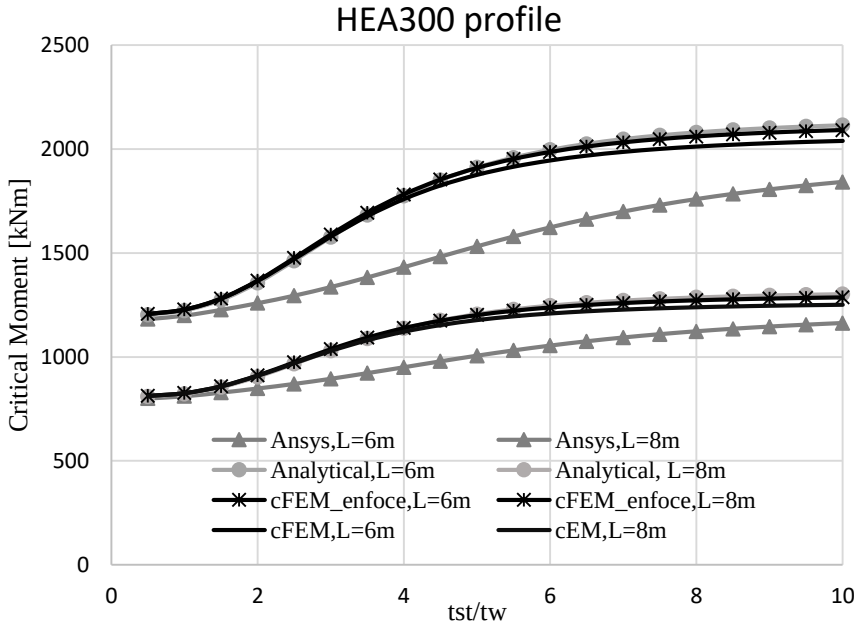

Figure 6: Critical bending moment, pinned-pinned supported member with two end-plates, cFEM_enforced, cFEM, Ansys FEM and analytical solutions, HEA300 profile

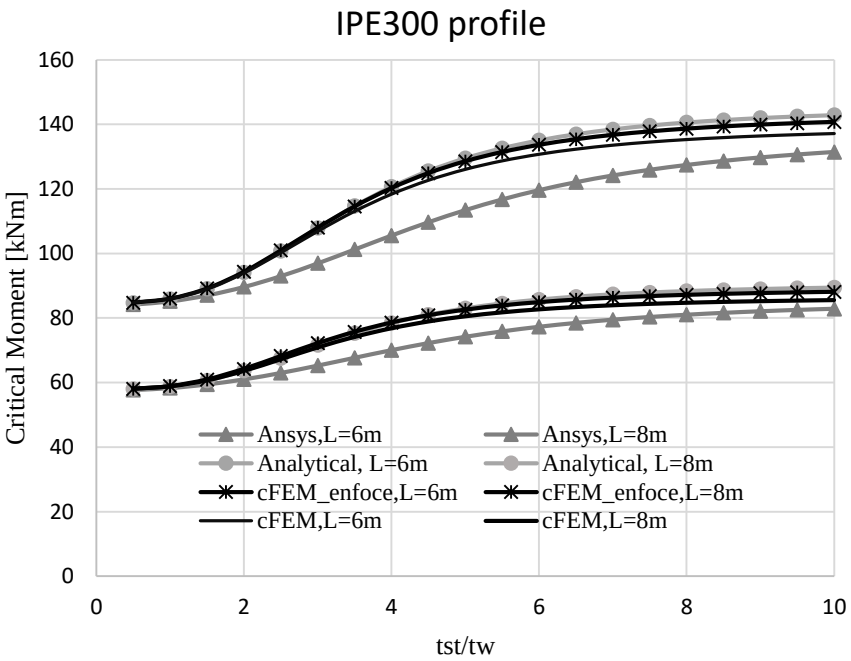

Figure 7: Critical bending moment, pinned-pinned supported member with two end-plates, cFEM_enforced, cFEM, Ansys FEM and analytical solutions, IPE300 profile

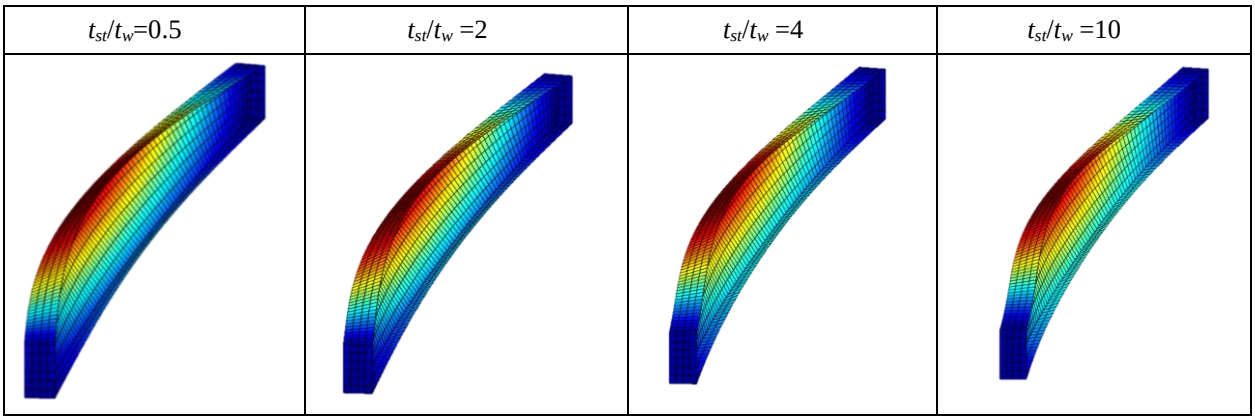

Figure 8: LTB buckling displacement shapes of the 6 m IPE300 member with two endplates

5. Conclusion

In this paper the effect of transverse plate elements on the lateral-torsional buckling of the doubly symmetrical I-section beams was studied. Particularly, transverse stiffeners and end-plates have been considered. Closed-form solutions were derived, using the energy method, for the critical moment of the beam for some simple support and loading cases. A number of numerical examples were presented; the analytically calculated results were compared to those from cFEM and Ansys shell finite element linear buckling analysis. The comparison showed the same tendencies in all the methods. The experienced differences between the results were explained.

It was proved that the transverse plate elements have significant effects on the torsional behavior, while negligible effects on the flexural behavior of the member. The two major effects on the torsional behavior were demonstrated by the numerical examples, too. A direct effect is due to the deformation of the stiffener. It can be explained – by using the logic of energy method – as follows: the deformation of the stiffeners increases the strain energy of the structure without changing its external energy, therefore the critical force is increased. The second effect is that the introduction of the stiffeners can (and typically do) modify the longitudinal distribution of the twisting rotations of the member which results in changing (in this case: decreasing) the critical load.
The numerical results suggest that the presence of the transverse plate elements has a beneficial effect on the critical moments. The increment due to the end-plates and/or transverse stiffeners is strongly dependent on the parameters of the problem, but even in practical situations the increment can be as large as 20-30%, which increment could be utilized in the design practice.

Acknowledgement

The presented work was conducted with the financial support of the K119440 project of the National Research, Development and Innovation Office of Hungary.

References

Ádány S. (2018a), Signature curve for general thin-walled members, In: Proceedings of the Structural Stability Research Council Annual Stability Conference 2018. Baltimore (MD), USA, April 10-13, 2018.

Ádány S. (2018b), Constrained shell Finite Element Method for thin-walled members, Part 1: constraints for a single band of finite elements, Thin-Walled Structures, Vol 128, July 2018, pp. 43-55.

Ádány S. (2019), Modal identification of thin-walled members by using the constrained finite element method, Thin-Walled Structures, Vol 140, 2019, pp. 31-42, https://doi.org/10.1016/j.tws.2019.03.029

Ádány S., Visy D., Nagy R. (2018), Constrained shell Finite Element Method, Part 2: application to linear buckling analysis of thin-walled members, Thin-Walled Structures, Vol 128, July 2018, pp. 56-70.

Ansys, Release 19.2, 2019.

Hoang T., Ádány S. (2020a), The effect of transverse stiffeners on the torsional buckling of thin-walled columns, Proceedings of the Annual Stability Conference, Structural Stability Research Council, Atlanta, Georgia, April 21-24, 2020. p 16.

Hoang T., Ádány S. (2020b), Torsional Buckling of Thin-Walled Columns with Transverse Stiffeners: Analytical Studies, Periodica Polytechnica Civil Engineering, 64(2), pp. 370–386, 2020, https://doi.org/10.3311/PPci.15137

Hoang T., Ádány S. (2020c), Constrained finite element method for thin-walled members with transverse stiffeners and end-plates, Thin-Walled Structures, 2020, https://doi.org/10.1016/j.tws.2020.107273.

Vlasov V.Z. (1961), Thin-walled Elastic Beams, National Science Foundation, Washington, DC, 1961.